Q&A-List to Concept- and Term-Specific Questions

Supplement to the 2025 Bridges Paper

"Reflected Motifs in Quasiperiodic Escher-Penrose Tilings"

Uli Gaenshirt[1] and Amrita Acharyya[2]

[1]Sculptor & Researcher, Nuremberg, Germany; uli.gaenshirt@gmail.com
[2]Department of Mathematics and Statistics, University of Toledo, Ohio 43606, USA; amrita.acharyya@utoledo.edu

Abstract

Escher-Penrose tilings are figurative or ornamental Escher tilings with a fivefold rotational symmetry, which completely fill the plane on the basis of the quasiperiodic Penrose tilings. We offer a chronological Q&A-list with additional detailled descriptions of terms and contexts in order to reach as many readers as possible.

Chronological Q&A-List to the 2025 Bridges Paper about Escher-Penrose Tilings

In many cases, the questions and answers of this Q&A-list refer to terms printed in *italics* in the paper, indicating that they are mentioned first at this point. The page numbers refer to the pages 1 to 8 of the pdf file of the paper, as well as the numbers of the Figures. The line numbers refer to the entire text of each page, without abstract, headings and captions. The Figures and Tables in this supplement are designated with capital letters to distinguish them from the Figures and Tables from the correspondant paper.

Page 1:

Line 5 – 12: *What are the features of the 17 crystallographic symmetry groups of the plane* ?

There are exactly 17 different periodic crystallographic symmetry groups of the plane. The main feature of these 17 groups are the translational symmetries, i.e. the identical, plane filling objects are lined up at equal distances on a straight line and therefore coincide with themselves when moved by one or multiples of these distances. With the exception of the group *p*1, all groups have additional features such as mirror axes, glide-mirror axes or centers with two-, three-, four- or six-fold rotational symmetries.

The chessboard grid in Figure 1(a) represents the symmetry group *p4m*, i.e. the grid has two classes of fourfold rotation, in the centers of the grey and white squares, one class of twofold rotation, in the corners of the squares, three classes of mirror axes, diagonally through the centers of the white and grey squares and alternately through the centers of the white and grey squares, and one class of glide-mirror axes that run along the vertical and horizontal grid lines.

The sheared rhombic grid on the right side of Figure 1(b) represents the group *cmm*, if the grey coloring is ignored. There are two classes of mirror axes, along the vertical and horizontal mirror axes of the individual rhombs, two classes of glide-mirror axes, the vertical and horizontal lines passing through the half-dividers of the rhombus edges, and three classes of twofold rotation, with their centers at the corners the rhombs, or at the centers of the rhombs, or at the half-dividers of the rhombus edges.

The dancer pattern on the left side of Figure 1(b) only has the two translational symmetries *t* and represents the symmetry group *p1*, the only group with no other symmetries.

The periodic female dancers are a periodically modified version of the quasiperiodic dancers which are shown on the pages 6 and 7 of the corresponding paper.

Line 13 – 15: *What is meant by a quasiperiodic tiling with a structural fivefold rotational symmetry* ?

It can be shown that a crystallographic (i.e. periodic) symmetry group with fivefold rotational symmetry cannot exist. Nevertheless, in 1973 Roger Penrose found tilings with an approximate fivefold rotational symmetry, but without translational symmetry as required in classical crystallography. These tilings are known today as Penrose tilings and are described as quasiperiodic, i.e. almost periodic.

Line 15 – 19: *What is a Penrose rhombus tiling* ?

The Penrose rhombus tiling consists of two proto-tiles, the thick and the skinny rhombs. Since the acute angles in a rhombus are equal, the thick rhombus has two acute angles of 72 degrees and two obtuse angles of 108 degrees. The angles of the skinny rhombs are 36 and 144 degrees.

In the thick rhombus the two legs of an acute angle must be distinguished from the legs of the opposite acute angle by edge marks so that the axis of symmetry of the thick rhombus is only the long diagonal. The axis of symmetry of a skinny rhombus lies on its short diagonal! The edge marks prohibit a 72 degree angle and a 108 degree angle of two thick rhombs from having a common leg. The same applies with a 36 degree angle and a 144-degree angle of two skinny rhombs. This means that the edge marks forbid periodically ordered arrangements. Conversely, they enforce a quasiperiodic structure with an approximate fivefold rotational symmetry. These restrictions imposed by the edge marks are today commonly called the matching rules.

Page 2:

Line 3 – 4: *What is the difference between Ammann lines, Ammann bars and an Ammann grid* ?

Robert Ammann was able to show that five sets of parallel lines can be laid across a rhombus tiling in such a way that they form identical constellations on all thick and all skinny rhombs. As there are only two different line spacings, the strips between two Ammann lines are today commonly called Ammann bars. The entire network of Ammann bars with five different orientations is known as the Ammann grid. Identical Ammann line segments drawn on the rhombs can be used as edge marks and thus represent the matching rules of the Penrose tilings.

Line 6 – 7: *What is a quasicrystal* ?

The discovery of metallic alloys with a structural fivefold rotational symmetry by Daniel Shechtman in 1984 was a sensation, because until then ordered nuclear structures with a fivefold rotational symmetry had been considered impossible. But Shechtman's x-ray diffraction patterns of his alloys left no doubt that he had discovered a nuclear structure with a long-range fivefold rotational symmetry.

Line 11: *What is the golden ratio, simply spoken* ?

The golden ratio τ is the ratio of the diagonal of a regular pentagon to its edge length! From the geometry of the regular pentagon follows: $\tau = 2\cos 36°$. Written as a root expression, this results in: $\tau = (1 + \sqrt{5})/2$. In decimal notation: $\tau = 1.61803398875...$, or in short: $\tau = 1.618...$.

We use the golden ratio τ to determine the ratio of the initial intervals $L_q/S_q = \tau$, where the capital letters stand for *long* and *short* and the indices q mean that these are the basic quasiperiodic lengths.

Line 12 – 13: *What is a Fibonacci chain* ?

A Fibonacci chain or a Fibonacci sequence is a quasiperiodic sequence of L and S intervals. The version we present here is symmetrical, with the exeption of the two intervals in the middle. This results from the substitution of the basic intervals L_q and S_q with reduced intervals L and S.

With the definition $L_q/S_q = L/S = \tau$ and $L_q/L = S_q/S = \tau^3$, the interval L_q can be substituted by the sequence LSLSL and S_q by LSL, keeping the corresponding length in both cases. The resulting sequence LSL<u>SL</u>LSL is a Fibonacci chain with eight elements. Please note that, unlike the other six elements, the two underlined elements in the middle are not symmetrical to the half-divider.

Line 13 – 14: *Can a Fibonacci chain of this type be extended at will* ?

By a continued and iterated substitution of L and S intervals, a Fibonacci chain can be expanded towards infinity, i.e. the next step is: L → L'S'L'S'L' and S → L'S'L', with L/L' = S/S' = $L_q/L = \tau^3$. This is followed by: L' → L"S"L"S"L" and S' → L"S"L". And then: L" → L'"S'"L'"S'"L'" and S" → L'"S'"L'". The LS sequence has 8 elements and the L'S' sequence has 34 elements. The L"S" sequence has 144 elements and the L'"S'" sequence has 610 elements. This is in accordance to the *Fibonacci numbers* F_6, F_9, F_{12} and F_{15}. The rule for the creation of the Fibonacci numbers is: $F_{n+2} = F_{n+1} + F_n$, with $F_1 = 1$ and $F_0 = 0$. $n \in \mathbb{N}_0$.

In a Fibonacci chain, a sequence appears maximum three times in a row, regardless of its length. For example: L'S'L'S'L'L'S'L'L'S'L'S'L'L'S'L'L'S'L'S'L'L'S'L'L'S'L'S'L'L'S'L'L'S'L'S'L'L'S'L' (note the underlined triple).

Line 15: *Why don't we use equidistant lines for a grid with a fivefold rotational symmetry* ?

In each periodic, crystallographic grid, the grid lines are equidistant and there exists only one mesh type. A checkered paper, for example, is created by equidistant vertical and horizontal grid lines and has only congruent, square meshes. De Bruijn's pentagrid consists of five families of periodic, equidistant, parallel lines and the five families of lines are rotated 36 degrees to each other. However, the pentagrid has an infinite number of meshes with different sizes!

Line 15 – 20: *How many grid meshes occur in an Ammann grid* ?

In contrast, the five line families in an Ammann grid have two spacings in quasiperiodic order because they are composed of five 1D-grids in which the order of the line spacings is given by a Fibonacci chain. Surprisingly, there are only eight different grid meshes in an Ammann grid. However, as described and illustrated in the associated paper, the five 1D-grids must be assymmetrically superimposed so that the central grid mesh has the shape of an irregular pentagon. The meshes of this type highlighted in color in Figure 2(b) are of particular importance, as it is possible to clearly assign one of the thick rhombs to each of these grid meshes, as shown in Figure 2(c). After filling the remaining gaps with skinny rhombs, the result is a flawless Penrose rhombus tiling!

Line 20 – 27: *What is a cartwheel and do cartwheels come in different sizes* ?

An Ammann grid constructed in the manner shown in Figure 2(b) is usually referred to as a *cartwheel.* The name is made clear by the fact that some centers of the colored grid meshes are marked with black dots: Their imaginary connections suggest the ten spokes of a cartwheel and its central hub. In Figure 2(c), a Penrose rhombus tiling is assigned to this Ammann grid. The different colors show the four nested rhombus cartwheels C_n: The red C_1, the blue C_2, the green C_3 and the yellow C_4. These four cartwheels correspond to the rhombic structures that can alternatively be created by the iterated classical substitution of a thick rhombus by reduced copies of the same, as described in [3] of our corresponding paper.

The cartwheels generated by the Ammann grid method are as follows: C_1, C_4, C_7, C_{10}, C_{13}, … , C_{3n+1}. The cartwheel C_{13} consists of more than half a million rhombs! This three-step substitution method is called *concordant*, because the substituted Ammann bars are a concordant subdivision of their initial predeccessor Ammann bars.

Line 28 – 33: *How can the symmetrical rhombs be compatible with the asymmetrical decorations* ?

The answer is that they are only partially compatible, i.e. the corner point structure is retained, while the mirror symmetry of the edges is abandoned. This also means that the two most common edge markers, as used in Figure 3(a), are not suitable for illustrating the principles of mirrored decorations of the rhombus tiling, as they cannot indicate a mirroring about the mirror line of a rhombus due to their own symmetry to this mirror line. In Figure 3(b), we will therefore introduce a third, less common marker type, called the Ammann notches, which break the symmetry of the rhombs with regard to reflections across the long diagonal in the case of the thick rhombus, and across the short diagonal in the case of the skinny rhombus. In the last two decoration examples of the paper we will show that even certain points of the corner point structure can be abandoned without giving up the relationship to the rhombus tiling.

Page 3:

Line 1 – 4: *How can edge marks control the matching rules for a local growth process* ?

The commonly used edge marks fulfill the locally acting matching rules in that they allow or forbid special constellations. The two marker versions shown in Figure 3(a) distinguish the two upper edges of the thick purple rhombus R_{id} from its lower edges and give the edges defined orientations. This is easy to see by de Bruijn's arrows and double arrows. Equivalently, the Ammann line segments are different at the upper and the lower edges and the orientation is given by their asymmetric placement on the edges. Each rhombus arrangement that is built with respect to the continuation of the Ammann line segments results in an Ammann grid, which shows that the matching rules are completely satisfied.

Line 5 – 9: *Are all neighborhood transformations h allowed by the matching rules* ?

Arranging the rhombs according to the matching rules prohibits periodic constellations. Conversely, the rules allow those neigborhoods of rhombs which generate a quasiperiodic order with an approximate structural fivefold rotational symmetry. Only allowed neighborhoods are defined as transformations h.

However, we can also see that the two usual markers in Figure 3(a) are mirror-symmetric to the long diagonal of a rhombus R, so that a mirrored, marked rhombus R^* seems to be identical to R. But we must distinguish R from its mirror image R^* if we want to describe a quasiperiodic rhombus arrangement with mirrored decorations in a generally valid form. This is possible with the asymmetric Ammann notches, that are used in Figure 3(b) to describe the transformation h_2^*.

Line 10 – 11: *What is designated by the index "id" in R_{id}* ?

The abbreviation "id" stands for "identity" and is used in the sense of a vertically oriented basic position. In Figure 3(a) top left, the point A_{id} of the purple rhombus R_{id} *is* shown in the origin (0, 0) of a coordinate system, with the top point T_{id} in (0, 1). The basic position with A_{id} in (0, 0) is necessary for an arithmetic description in the complex plane $\mathbb{C}$. There, the coordinates of the point T_{id} should be written as (0, i).

Line 11 – 14: *What is the definition of the transformation h_j and h_j^{-1} and what is meant by the stars* ?

A transformation h_j always refers to the dominant thick rhombus R_{id} and describes the movement of a copy of R_{id} in relation to the initial position of R_{id}. In Figure 3(a), these movements are geometrically defined by a rotation around a suitable point T, V or W. The inverse transformations h_j^{-1} describes a reverse direction of rotation. The five transformations h_j are marked by the indices $j \in \{1, 2^*, 3, 4^*, 5)$. The star in h_2^* and h_4^* denotes, that R_{id} is first mirrored about its long diagonal before being clockwise rotated by 36 degrees about the points W_2 or W_4! However, the reflections are not visible in Figure 3(a), as the edge marks of the thick rhombs R are mirror symmetric to the long diagonal of R, like the rhombs themselves. The marked skinny rhombs R_s are mirror symmetric to their short diagonal.

Line 15 – 19: *Why are the Ammann notches in Figure 3(b) described as "symmetry-breaking"* ?

In Figure 3(b) it can be seen that the notches on the left side of the purple rhombus R_{id} are outside its edges and on the right side inside of them, i.e. the notches are not symmetrical to the long diagonal of the rhombus R. Nevertheless, they allow the transformation h_1 in the same way as the marks in Figure 3(a). But the usual edge marks in Figure 3(a) would also allow the transformation h_1 using one rhombus R_{id} and another rhombus R^*. The Ammann notches shown in Figure 3(b) would force that the rhombus R_{id} is not mirrored during a transformation h_1.

In contrast, the transformations h_2^* in Figure 3(b) show that a mirroring of R_{id} is necessary to match the reflections of the decorations shown in Figure 3(c). This presupposes that the skinny rhombus R_s must have suitably shaped notches. As described in detail in the corresponding paper, the Ammann notches of the skinny rhombs are extracted from the inside of a thick rhombus by means of triangles, mirrored and then inserted into the skinny rhombus at the corresponding point. Now the Ammann notch of the skinny rhombus only allows a mirrored thick rhombus R^* to be attached to the skinny one.

Line 20: *Is there a principal difference between the Ammann notches and the animal decorations* ?

There is no difference in principle. Each Ammann notch can be clearly assigned to a deformed edge of an animal decoration, i.e. the outlines of the animals can be regarded as Baroque-style Ammann notches. However, the upper and lower edges must be different and the respective right edge must match the left edge exactly. In Figure 3(c), the transformation h_2* is split into its components using the example of the animal decoration. The mirrored reduced swan-dinos represent the reflection of the rhombus R_{id} at its long diagonal, whereby the mirror images are shown side by side to avoid overlaps. The mirrored swan-dino is then clockwise rotated 36 degrees around the point W_2. This rotation represents the transformation h_2. The mirroring and the rotation together result in the transformation h_2*. The blue mirrored rhombus R* is therefore labeled $h_2^*(R_{id})$. The designation $h_2(R_{id}^*)$ would of course be just as right.

Line 21 – 27: *Why are there only two mirroring versions among the five transformations h_j* ?

In the seven lines below Figure 3 you will find a description of the geometric rotations shown in Figure 3(a). In the transformation h_3, a mirroring by the Ammann notches is prohibited for the same reasons as described for h_1 above. Reflections by the (optional) pair of skinny rhombs in the transformation h_5 cancel each other out! I.e. a mirroring of a thick rhombus R_{id} can only be realized in the transformations h_2* and h_4* via a single skinny rhombus R_s. The transformations h_2 and h_4 are not used in our paper.

Line 28 – 30: *Why are arithmetic and geometric descriptions of the transformations h_j different* ?

In the geometric illustrations in Figure 3(a), the rhombs R_{id} are always arranged vertically and can all be considered to be placed in a cartesian coordinate system with the point A_{id} in the origin. In this geometric illustrations each transformation h_j is completely described by a rotation around a pivot point T, V or W, without any additional shifting. A mirroring before a rotation is possible, but not visible in Figure 3(a).

For the arithmetic description of a rotation, the center of rotation must be the center of the complex plane $\mathbb{C}$. Therefore, the center point A_{id} of the rhombus R_{id} must be placed in the origin. During each rotation of R_{id}, the center point A_{id} remains at the origin. On the other hand, in the geometric versions of the transformations h_j, where R_{id} is rotated around the points W_2, W_4, V_{id} or T_{id}, the points A_{id} are shifted. This can be seen in the example of the dashed yellow arrow in the transformation h_1 in Figure 3(a) top left. From this follows that in the algebraic description of the transformation h_1, the point A_{id} still has to be shifted along the dashed yellow arrow. Consequently, all numbers z of the rotated rhombus R_{id} must be shifted in this direction with the length l of the dashed yellow arrow, with $l = 2\sin(\pi/5)$. Only then, the algebraically transformed rhombus corresponds to the geometrically transformed rhombus if the two transformations refer to the same initial rhombus R_{id}!

In the transformations h_2* and h_4* in Table A, the reflection of the rhombus R_{id} about the y-axis is described by a conjugation of the numbers z ($z \rightarrow \bar{z}$, which induces a reflection about the x-axis), together with an additional rotation with π (i.e. about 180 degree). The needed shift by the length l must take place after mirroring and rotating the numbers z. For the transformation h_5, the shift length is likewise l. Only for the transformation h_3, the shift length is reduced to $s = \tau^{-1} l$.

Table A: *The arithmetic definitions of the transformations h_j in the complex plane including h_2* and h_4*.*

R_{id} is defined by $T_{id}\ (0, i)$, $A_{id}\ (0,0)$ and $V_{id}\ (0, -i\tau^{-1})$	$h_1(z) = z \cdot \omega_2 + l \cdot \omega_1$	Left: Classic transformations h_j. Below: Substitution of h_2 and h_4 by h_2* and h_4*, which mirror the rhombus R_{id} on its long diagonal.
The rhombus edge length a_R is here scaled to: $a_R = 1$	$h_3(z) = z \cdot \omega_8 + s \cdot \omega_9$	
The inverses: $h_j^{-1}(h_j(R_{id})) = R_{id}$, $j \in \{1, 2^*, 3, 4^*, 5\}$	$h_5(z) = z \cdot \omega_2 + l \cdot \omega_8$	
$z \in \mathbb{C}$, $\omega_k = \cos(k\pi/5) + i \sin(k\pi/5)$, $k \in \{0, 1, \ldots 9\}$	$h_2(z) = z \cdot \omega_9 + l \cdot \omega_1 \quad \rightarrow \quad h_2^*(z) = \bar{z} \cdot \omega_4 + l \cdot \omega_1$	
$l = 2\sin(\pi/5)$ and $s = \tau^{-1} l$ with $\tau = (1+\sqrt{5})/2$	$h_4(z) = z \cdot \omega_9 + l \cdot \omega_8 \quad \rightarrow \quad h_4^*(z) = \bar{z} \cdot \omega_4 + l \cdot \omega_8$	
Please note: A conjugated complex number $\bar{z}$ represents a mirror reflection of z about the real x-axis. A reflection of z about the imaginary y-axis is given by: $z \rightarrow \bar{z} \cdot \omega_5$, where ω_5 is taken into account by replacing ω_9 with ω_4.		

Page 4:

Line 1: *In what way has the Penrose Kite & dart tiling anything to do with the rhombus tiling* ?

The mutual derivability of the Penrose rhombus tiling and Penrose kite & dart tiling is based on the fact, that their prototiles can be assambled by the same triangles, an acute golden triangle, with an apex angle of 36 degrees and base angles of 72 degrees, and an optuse golden triangle, with an apex angle of 108 degrees and base angles of 36 degrees.

In the rhombus tiling, the thick rhombus R consists of two acute and two obtuse golden triangles. The skinny rhombus R_s is composed of two acute golden triangles with a common base.

In the kite & dart tiling, the kite K consists of two acute golden triangles with a common leg and a common apex. The dart tile D is made of two obtuse golden triangles, which also have a common leg and a common apex and whose common base corner should be designated as the top point T.

Line 1 – 6: *How can it be that the decorations of two different tilings have the same order* ?

As the corner point structure of the animals in Figure 4(a) is assigned to the corner points of the basic triangles, the animals have exactly the same order in both tilings. The common base corner T of the dart D corresponds to the top point T of the thick rhombus R. Therefore, they have an equivalence relationship with one another. Both tiles play the dominant role in their tiling, in that the transformations h are related to them. But the center point A of the thick rhombus R, which plays an important role in the algebraic definition of the transformations, is not contained in the dart tile D at all. Nevertheless, the point A must be assigned to D in any case.

Although the proto-tiles of both tilings consist of exactly the same golden triangles, the two crossed-out white arrows in Figure 4(b) also show that a thick rhombus R cannot be composed of one kite and one dart tile. Consequently, the Ammann notches both tiles do not match either in this way.

Line 7 – 11: *Can two successively executed transformations correspond to another transformation* ?

Yes, that is possible. In Figure 4(b) of the paper, a dashed, acute golden triangle can be seen in the center. Its corner points are the three points A, which are assigned to the purple dart D, to the mirrored yellow dart D^* and to the turquoise dart D. The two legs of the dashed triangle correspond to the movement of point A in the transformation h_2^* (purple D to mirrored yellow D^*) and h_4^* (yellow D^* to turquoise D), while the shorter base of the triangle corresponds to the movement of A in the transformation h_3 (purple D to turquoise D). The dashed triangle therefore not only shows that the successive execution of h_2^* and h_4^* corresponds to the transformation h_3, but also that the reflections of the two mirroring transformations cancel each other out.

Line 12 – 21: *How can quasiperiodicity be visualized clearly for non-specialists* ?

The arrangement of the animals in Figure 5(a) is visually interesting, but probably incomprehensible to all non-specialists. The quasiperiodicity of the kite & dart cartwheel in Figure 5(b), which has an equivalent relation to the animals, is also difficult to understand. Nevertheless, the tiling in Figure 5(b) is because of its coloring particularly suited to visualize the principle of quasiperiodicity in a decomposition into five one-dimensional (1D) partitions.

For the clarity of presentation, only the kites K are observed in the Figures 5(d-h). In order to show their linear alignment, a family of parallel Ammann lines is additionally drawn in each 1D-tiling. The lines do not intersect the K tiles as they belong to a larger tiling.

Since the five 1D-structures are very similar to each other, especially in larger contexts, it is obvious that their superposition comes very close to a structural fivefold rotational symmetry.

However, this approach also has scientific relevance, as the quasiperiodic row-shaped arrangement resembles a crystalline row-shaped structure, even if there is no translational symmetry as in crystals. But the row-shaped order also explains the tenfold symmetrical X-ray diffraction patterns of the quasicrystals, as the X-rays are always refracted at atomic rows before they produce the structure image.

Page 5:

Line 1 – 6: *Is there a connection between the historical and the quasiperiodic Girih patterns* ?

In the Girih patterned quasiperiodic hexagon boat (HB) tiling, which is shown in Figure 6(a) and 6(b) in the associated paper, the *H* and *B* tiles have geometric shapes, which correspond to the historical used Girih stemcils or can be assembled from them. With the uncolored tiles in Figure A(a), we could create an infinite number of patterns, both periodic and quasiperiodic, as well as freely composed versions adapted to architectural conditions, as they can be seen on historical buildings, especially in the Middle East.

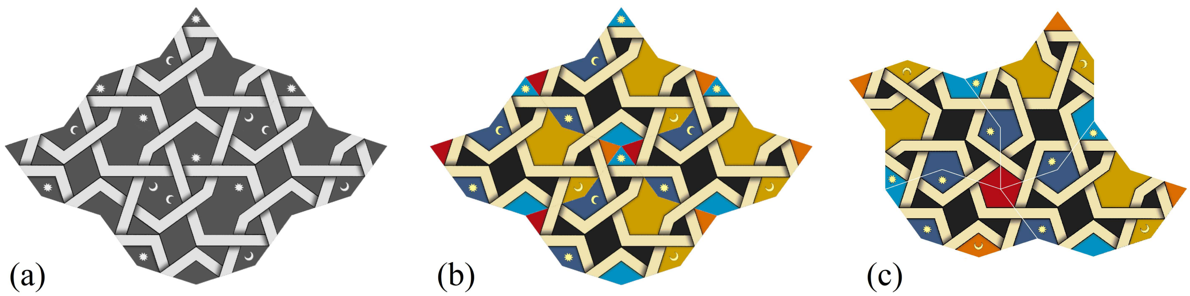

Figure A: *(a) Four periodically arranged uncolored boat tiles B. (b) The same arrangement with color-coded tiles, ignoring the rules. (c) Color coded tiles in accordance to the quasiperiodic matching rules.*

In the colored version in Figure A(b), the four periodically arranged B tiles are clearly visible. However, this periodic arrangement contradicts the quasiperiodic matching rules which force that only same colors can be placed next to each other. The three *B* tiles and the one *H* tile in Figure A(c) show an arrangement that is composed in accordance to the color-coded quasiperiodic matching rules.

Line 7 – 12: *Is a Penrose HB tiling also possible without mirroring or turning the tiles on its back* ?

In the Penrose *HB* tiling the reflections of the tiles or the turns on their backs are a mandatory prerequisite for the gapless filling of the plane. because only the transformations h_2* and h_4* create the corresponding gaps for the *H* and *H** tiles between the *B* and *B** tiles. The transformations h_2 and h_4 lead to 36 degree gaps between the *B* tiles, which cannot be filled with *H* tiles!

Line 13 – 15: *Why are the edges of the H and B tiles identical to the edges of the H* and B* tiles* ?

This is due to the spatial over and under of the Girih strands. If you look from the inside of a tile at one of its edges, the strand coming from the left always overlaps the one coming from the right. If you turn the tile to its back, the strand coming from the right now comes from the left, but it also becomes an overlapping strand when you have turned it to the back. i.e. nothing has changed,

In Figure A(b) and A(c), the identical edges of the different tiles are clearly visible. There you can also see that the strands of the Girih pattern all continue in a straight line across the common edge, always overlapping each other in the same way.

Line 16 – 20:

The sun-moon rule is an addition to the color coded matching rules. The prohibition of two suns or two moons in one color field is in a certain sense an urgent warning that the next step is a dead end.

The situation is comparable to that when two skinny rhombs, marked with de Bruijn's arrows and double arrows, are placed together with their single arrows. This is not explicitly forbidden, but it creates a gap into which two single arrows point. However, such a tile arrangement is called a dead end, as there is no way to fill the gap.

The double sun and the double moon are a practical way to minimize frustration when puzzling the tiles, because the dead-end situations in the *HB* tiling are much more difficult to recognize than in the marked rhombus tiling.

Page 6:

Line 1 – 7: *Is the outline of the periodic dancers really different from the quasiperiodic dancers* ?

Figure B(a) shows four of the periodically conceived female dancers from Figure 1(b) of the associated paper in a larger scale. We can see that their slightly curved outlines fit together very precisely in the periodic arrangement shown here.

In contrast, we can see that the four quasiperiodically conceived dancers in figure B(b), which have exactly the same outlines as the dancers in Figure 7(a) and Figure 8 from the associated paper, do not fit together in the periodic positions shown here.

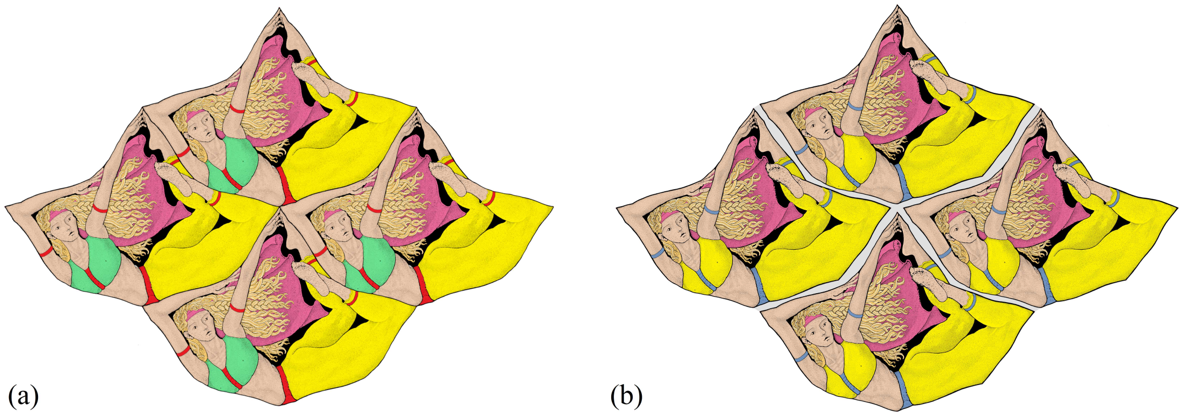

(a) (b)

Figure B: *(a) Periodic dancer pattern. (b) Quasiperiodically conceived dancers in periodic positions.*

Conversely, the periodically arranged dancers from Figure B(a) would not fit together everywhere in the large quasiperiodic arrangement in Figure 8, although the local centers with fivefold rotational symmetry could also be assembled with the periodically conceived female dancers. However, a further connection between these local rotation centers would not be possible, not even by reshaping the edges ot the male dancers. All outlines of the dancers in Figure 8 must be as they are in order to generate a quasiperiodic structure with a fivefold rotational symmetry!

Line 8 – 14: *Why are the unmirrored dancers in Table 1 not shown in the standard orientation* ?

In the creation of the ballet dancers, the artistic edge design corresponds best to the technically necessary edge modification when the knees of the female dancers coincide with the points T of the tiles B and B^*. Since the central female dancer in the cartwheel, which is supposed to be an unmirrored B tile, would thus be upside down, the entire cartwheel is rotated by 180 degrees.

This means that we have prioritized the artistic decision on a suitable central dancer position over pragmatic considerations, even if we have made it a bit more challenging to understand Table 1.

Page 7:

Line 1 – 15: *Are there several outlines with fivefold rotational symmetry in the HB cartwheel* ?

Since the *HB* cartwheel is defined up to a size that goes towards infinity, it can be shown that the number of outlines with a fivefold rotational symmetry also goes against infinity.

One of the most artistically interesting outlines is larger than the cartwheel C_3 in Figure 8 but smaller than the cartwheel C_4, which is represented by the complete rhombus tiling in Figure 2(c). The almost circular arrangement without rotational symmetry consists of a total of 110 dancers and is enclosed by 30 female dancers! We show you this arrangement on the following page.

This version of the ballet dancers will also be on display in a large size with a diameter of more than one and a half meters at the Bridges 2025 Exhibition of Mathematical Art and Design.